EAI Endorsed Transactions
on Energy Web
Research Article EAI.EU

Investigation on ANFIS-GA controller for speed control of a BLDC fed hybrid source electric vehicle

P. Jagadish Babu[1] and A. Geetha[2,*]

[1, 2] Department of Electrical and Electronics Engineering, College of Engineering and Technology, SRM Institute of Science and Technology, Kattankulathur, Chengalpattu, Tamil Nadu 603203, India

Abstract

The BLDC (Brushless DC Motor) is utilized in electric vehicles, space missions, and mechanical applications. Neural Network Inference System reduces torque ripple for hybrid electric vehicle (PV-Battery) along with BLDC drive to achieve efficient speed performance and stability. A hybrid input source methodology is thus put forwarded to drive the stator currents giving exactly the expressed electromagnetic torque and counter-EMF harmonics. The torque and speed control technique are directed to neural network interference system, and H6 Voltage Source Inverter (H6 VSI) drives BLDC with a gate pulse signal. We examine how an ANFIS-GA torque controller may eliminate BLDC torque ripples under uninterrupted hybrid power supply in this work. MATLAB (Simulink) results show that Genetic Algorithm (GA) improves training of ANFIS better with varying set speed conditions. The ANFIS-GA controller outperforms challenging controllers under various BLDC motor driving load conditions, proving its efficiency.

Keywords: PV, Battery Pack, ANFIS, GA, H6 VSI, BLDC Motor

Received on 02 November 2023, accepted on 21 January 2024, published on 29 January 2024

doi: 10.4108/ew.4965

*Corresponding author. Email: geethaa2@srmist.edu.in

1. Introduction

With the increasing popularity of electric vehicles (EVs) as a sustainable transportation solution, the development of efficient and reliable charging systems is of paramount importance. Among the various components of an electric vehicle, the motor plays a critical role in propulsion, and the BLDC has emerged as a preferred choice due to its high efficiency and excellent torque characteristics [1], [2]. It was reported that the costs of operating an electric vehicle are lower than the costs of operating a regular gasoline-powered vehicle. Because electricity is typically more affordable than either gasoline or diesel, this results in lower overall expenses for fuel. EVs also require less maintenance than traditional vehicles since they have less expensive components [3], [4]. It has been stated that the growth of infrastructure for charging electric vehicles has been a significant factor in the rising popularity of electric automobiles. The rapid growth of fast-charging stations has further reduced charging times of the vehicle which leads to guiding EV more applicable for long-distance travel. Efficient battery charging is eventual significance for electric vehicles (EVs) as it directly impacts their driving range, overall performance, and user experience [5], [6]. The driving range of an EV is determined by the capacity and efficiency of its battery. The increasing demand for electric vehicles (EVs) has led to significant advancements in motor technology, with BLDC emerging as a popular choice for EV propulsion systems [7].

BLDC motors offer high efficiency, compact size, and excellent torque characteristics, making them suitable for electric vehicle applications. Due to its high torque density and drive required a modest controller for its control, BLDC motors are currently being evaluated for a wide range of EV applications [8], [9]. Using back EMF data collected from a brushless DC motor, we show how

each stage of the design process works in practice. Torque-ripple-free operation is possible in principle for BLDC with a sinusoidal back electromotive force stated by Dasari, et al. (2022) [10]. However, motor design and controller execution can still produce parasitic torque ripples. In this study, we take a methodical look at how motor controller constraints might cause torque ripples in a BLDC drive [11], [12], [13]. It explains the limitations of the current sensors and the pulse width modulation switching in the inverter [14], [15]. Methods have been developed to analyze and compute torque ripple from each of these sources. The following methodology can increase a BLDC motor torque density: Increasing either the amount of the measured current or the intensity of the magnetic field, or both, are all viable options. Increasing the current results in a higher copper loss in the windings and using stronger magnetic material to increase the intensity of the magnetic field raises the system's price and complexity. The primary difficulty, then, is to boost the current without increasing the copper loss in the windings or the strength of the magnetic field, both of which would raise the system's price and complexity. Furthermore, the torque ripple must be kept to a minimum, especially at low speeds, for most of the applications.

In Section II, we go into the concerns with the mathematical model of hybrid source fed BLDC motor. The proposed method for rotor position ANFIS-GA controller is described in Section III. In this section IV, we also present the simulation of ANFIS-GA controller that establishes the improvement in the BLDC drive's torque density and contains thorough hardware studies. The experimental validation of the BLDC drive is presented. In Section V, includes the in-depth research conclusion.

2. Mathematical model of hybrid source fed BLDC motor

We assume that the hybrid PV-Battery input system provides an efficient voltage to drive BLDC motor drive. In a BLDC-based electric vehicle (EV), both the inverter and hybrid Photovoltaic-Battery source system play vital roles in ensuring efficient operation and maximizing energy utilization. The inverter acts as the bridge between the vehicle's power source, typically PV and battery, and the BLDC motor drive. By controlling the frequency and amplitude of the AC output, the inverter enables defined control over the motor's speed and torque, resulting in smooth acceleration, deceleration, and regenerative braking.

The following equation presents the voltage that must be present across the motor winding to have a balanced system and symmetrical winding. The mathematical model may be stated by using the following equation when Kirchhoff's defined voltage law is applied to 3phase stator loop winding circuits illustrated in equation (1), (2), (3).

$$V_p = R_p\, i_p + L_p \frac{di_p}{dt} + M_{pq} \frac{di_q}{dt} + M_{pr} \frac{di_r}{dt} + e_p \quad (1)$$

$$V_q = R_q\, i_q + L_q \frac{di_q}{dt} + M_{qr} \frac{di_p}{dt} + M_{qr} \frac{di_r}{dt} + e_q \quad (2)$$

$$V_r = R_r\, i_r + L_r \frac{di_r}{dt} + M_{rp} \frac{di_p}{dt} + M_{rq} \frac{di_q}{dt} + e_r \quad (3)$$

V_p, V_q, V_r represents the voltage across phase of the BLDC motor, R_p, R_q, R_r denotes the stator winding resistance, i_p, i_q, i_rdetermine the phase current of the P,Q,R winding of BLDC motor, L_p, L_q, L_r Signify the self-inductance of the BLDC motor, M_{rp}, M_{qr}, M_{pq} illustrate the stator winding mutual inductance as shown in below equation (4).

$$\begin{bmatrix} L_p & M_{pq} & M_{pr} \\ M_{qp} & L_q & M_{qr} \\ M_{rp} & M_{rq} & L_r \end{bmatrix} \frac{di}{dt} \begin{bmatrix} i_p \\ i_q \\ i_r \end{bmatrix} = \begin{bmatrix} V_p \\ V_q \\ V_r \end{bmatrix} - \begin{bmatrix} R_p & 0 & 0 \\ 0 & R_q & 0 \\ 0 & 0 & R_r \end{bmatrix} - \begin{bmatrix} e_p \\ e_q \\ e_r \end{bmatrix} \quad (4)$$

The speed, back-EMF, and current waveforms that are being applied all have an effect on the electromagnetic torque that is generated by this three-phase BLDC motor. Therefore equation (5), represented to express the instantaneous electromagnetic torque is

$$T_{em} = J \frac{d\omega_r}{dt} + B\omega + T_L \quad (5)$$

Where, $\omega, B, J,$ each represent a different component of the motor's angular velocity, frictional coefficient and moment of inertia respectively. The load torque is denoted by T_L. Therefore equation (6), to express the instantaneous electromagnetic torque is.

$$T_{em} = \frac{1}{\omega_m} (e_p i_p + e_q i_q + e_r i_r) \quad (6)$$

3. Proposed rotor position ANFIS-GA controller

The ANFIS torque motor controller was designed with the significant objective of increasing torque density over standard BLDC motors. To attain that significant outcome, the stator windings need to be generated with the efficient current waveform.

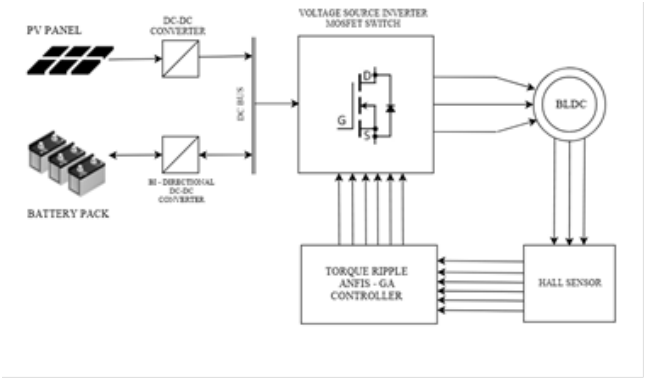

Figure 1. Enhanced BLDC drive controller using ANFIS-GA

As shown in Figure 1, the hybrid input source generates power to the conventional three-phase H6 inverter that powers the BLDC motor. Whereas the inverter switching states are determined by the data received from three hall sensors that track the rotor condition and point position. Evaluated that the proposed motor generates a nearly calculated back EMF with an optimal efficiency for producing optimum torque controller signal.

The design of the ANFIS-GA Controller is greatly impacted by the accessibility of knowledge methods and knowledge bases. A significant impact on ANFIS-GA logic applications is provided by these two characteristics. However, genetic algorithms apply the principles of genetics and natural selection to the process of optimizing computer searches and optimizations as shown in Figure 2. Natural selection and the process of evolution are incorporated into genetic algorithms. The primary objective of the genetic algorithm is to simulate natural selection, which is the hypothesis that only the fittest and healthiest individuals would be able to continue living and pass on their characteristics. The answers are presented in the form of chromosomes via genetic algorithms. These chromosomes serve as the standard by which fitness is measured. The output membership functions of Mamadani are presented as a scattered set, whereas the Sugeno represents Set linear function.

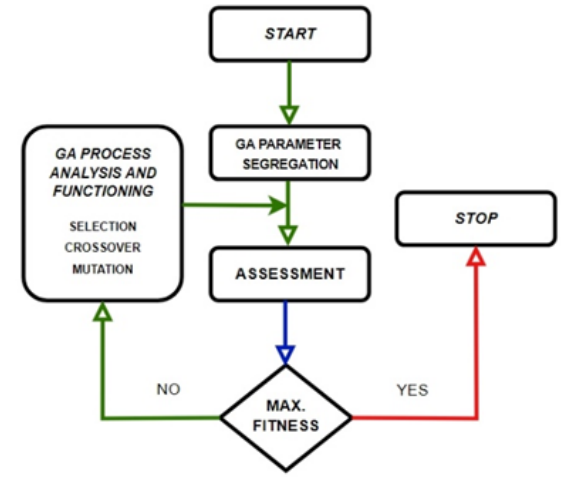

Figure 2. GA parameter segregation flow chart

The linear output membership function makes defuzzification much easier to accomplish. In GA, the initial chromosome population is generated at random, and the chromosomes of following generations, also known as kid chromosomes or offspring chromosomes, are given the name kid chromosomes. The goal of using superior parents in reproduction is to improve the chances of offspring reaching their full potential. Natural selection leads to the advancement of chromosomes that are more robust while the less robust ones are eliminated. It is possible for the level of training to improve ANFIS performance and the below equation (7) states the Gaussian membership functions.

$$\mu_{Ai}(x) = \frac{1}{1+\left(\frac{x-b_i}{a_i}\right)^2} \tag{7}$$

3.1 ANFIS - sugeno structure

A Sugeno fuzzy inference system is the initial base for a type of artificial neural network termed as an ANFIS (adaptive neuro-fuzzy inference system). A single framework constructed with both neural networks and fuzzy logic, as a result inference system is efficiently collected fuzzy IF–THEN rules, and these rules are able to learn nonlinear functions and approximate their values. This system attained an approximate nonlinear functions frame, generated by the rule of determined evaluating capabilities. As a result, ANFIS is regarded as a universal estimator which defines input and output layer in Figure 3. It is possible to employ the best parameters that were obtained by the genetic algorithm in order to use the ANFIS in the most effective and optimal method possible.

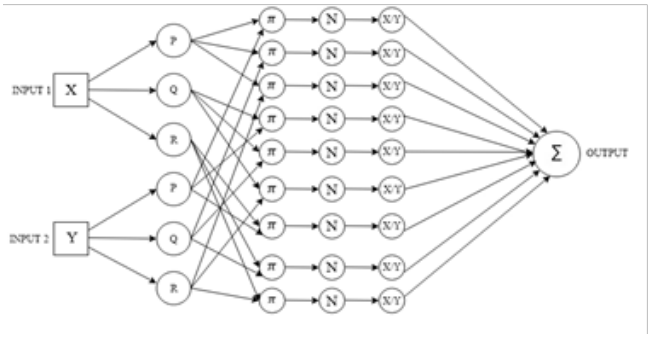

Figure 3. ANFIS structure

We are going to simplify things by assuming that the fuzzy inference system considered only single output, z, and dual inputs, x and y. The following is an example of a collective set of rules that has dual fuzzy if-then rules and is applicable to a first order Sugeno fuzzy model as formulated in equation (8), (9):

$$\textbf{Framed rule 1: } x = f_1 = p_1 + q_1 + r_1 \quad (8)$$

$$\textbf{Framed rule 2: } y = f_2 = p_2 + q_2 + r_2 \quad (9)$$

Layer 1 Process

In this layer, equation (10), (11) states that every i^{th} node has a corresponding function that adapts to its surroundings.

$$O_1 = \mu_{Ai}(x) \quad (10)$$

$$O_2 = \mu_{Bi-2}(y) \quad (11)$$

Layer 2 Process

Each node in this layer is defined as a fixed rule node with the input X value and Y value identifiers. The output of these nodes generates efficient form as shown in equation (12) for all the input X and Y signals:

$$O_2 = \omega_i = \mu_{Ai}(x)\mu_{Bi}(y) \quad (12)$$

Each node's output calculates a rule to trigger a result. The node function in this layer can be any additional T-norm operator that implements fuzzy.

Layer 3 Process

Each individual node in this layer is a fixed parameter node, indicated by the letter N. As formulated in equation (13), the i^{th} node calculates the fraction of the total firing strength that is resultant to the i^{th} rule.

$$O_3 = \overline{\omega_i} = \frac{\omega_i}{\omega_1 + \omega_2}, \quad (13)$$

This layer's outputs are defined as normalized firing strengths for minimal outcome.

Layer 4 Process

Each i^{th} rule node in this layer is designated as an adaptive node with the following node function: where N value is the normalized firing strength from the previous layer $p_i(x), q_i(y), r_i$ are the parameters for this node as shown in below equation (14).

$$O_4 = \overline{\omega_i} * f_i = \omega_i(p_i(x) + q_i(y) + r_i) \quad (14)$$

The parameters located at this level are referred to as consequent parameters.

Layer 5 Process

There is always one node (represented by the z value) in this layer 5 processing. This node calculates the collective output, which is equal to the sum of all inputs as insisted in equation (15):

$$O_5 = \sum_i \overline{\omega_i} * f_i = \frac{\sum_i \omega_i f_i}{\sum_i \omega_i} \quad (15)$$

As a result, we have developed an adaptive network that performs in a mode that is corresponding to that of an ANFIS Sugeno fuzzy model.

3.2 Design of ANFIS-GA controller for BLDC drive

In the following, ANFIS-GA controller simulated for driving the BLDC motors will be discussed.

Stage 1

The selection of inputs is considered under ANFIS-GA controller receives as inputs the RPE (rotor position error), rate of change in error (ROE), and CS (control signal).

Stage 2

Hall sensor input variables are selected. The following input variables are utilized in the description of the input variables: All the way up to the positives: Z (zero value), PS (positive assumption small value), PB (positive assumption bigger value), NS (negative assumption smaller value), and then NB (negative assumption bigger value).

Stage 3

Select the membership functions that are linked to the inputs. The utilization of Gaussian membership functions is active to determine the X and Y input variables.

Stage 4

The fuzzy model of the enhanced controller is selected as the further step. One of the initial orders of fuzzy modeling this arrangement takes use of the computational efficiency obtainable by Sugeno.

Stage 5

Step involves the compiling of input X value and Y value training data pairs for the enhanced controller. While

learning how to function properly, the ANFIS-GA controller utilizes training data pairings consisting of the rotor's position error (RPE), rate of change in error (ROE), and CS (control signal).

Stage 6

The fundamental assumptions of the ANFIS-GA controller as well as its output parameters are optimized.

3.3 Training process of ANFIS-GA controller

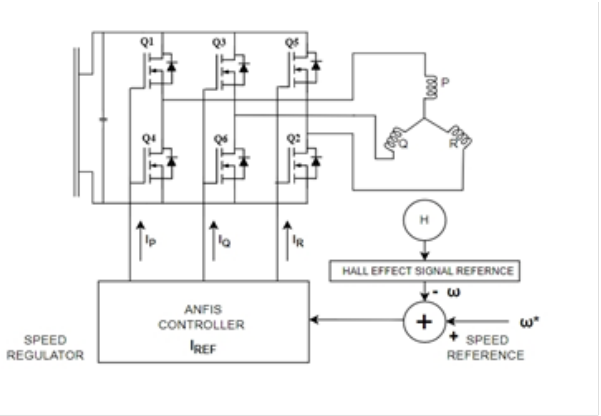

Figure 4. Hall-Effect reference signal fed ANFIS-GA controller - current reference signal

The process of simulation modelling the ANFIS-GA controller involves various stages of processing, one of the most significant things is the attainment of input X and Y values for training data pairs. A Hall Effect reference signal fed ANFIS-GA controller - current reference signal is illustrated in Figure 4. For the determination of simulating the ANFIS controller, the input and output data from a hall sensor reference controller are utilized. Using an ANFIS-GA controller, the input-output data set is managed in a closed loop to prevent the system from becoming overloaded. The ANFIS-GA controller considers both the input error signal (ES) and the ROCE (rate of change of error) from the BLDC motor as inputs. Training procedure can start as soon as the input membership functions have been configured successfully. After the training method has been completed, the ANFIS-GA controller is able to be validated with the use of the training data. The Hall sensor HP, HQ, HR reference value are ordered with the input layer at the top. The following layer that is added is determined as the input function layer (Input X, Y). Whereas the inference engine layer, which is located on the third portion, connects the inputs and the outputs by making use of the AND operator. The output layer is the very last one, and it is responsible for optimizing and generating effective outcomes.

3.4 ANFIS-GA controller fed inverter.

ANFIS-GA controller was designed with the objective of increasing torque density over BLDC motors. To attain a significant output, the stator windings need to be generated with the efficient current waveform and respond to efficient gate signal. As in Figure 4, ANFIS-GA controller fed three phase voltage source H6 inverter which provides power to drive the BLDC motor. The inverter switching conditions are determined by input data from three hall sensors that track the rotor point position. Therefore, the proposed motor generates a nearly calculated back EMF with an optimal efficiency for producing optimum torque controller signal.

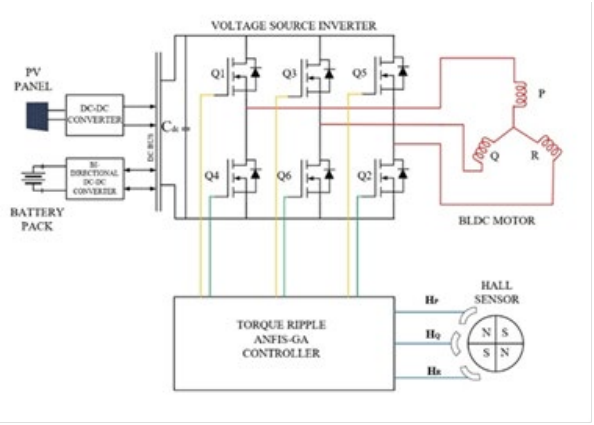

Figure 5. ANFIS-GA controller fed voltage source inverter

Hybrid power input sources are provided by the proposed controller fed to H6 inverter based on the power balance among the input terminal ports, as shown in Figure 5. Figure depicts the operating gate signals for higher leg MOSFET Q1, Q3, Q5 and lower leg MOSFET Q2, Q4, Q6. The desired switching frequency of the H6inverter is used to compare a constant (duty cycle) for each input source with a trapezoidal signal (reference trapezoidal) with that same frequency. If the trapezoidal pulse value is less than the duty cycle, the switch will be in the OFF position; otherwise, it will be in the ON position. The conduction of switches Q1 Q3 and Q5 is forward to that of switches Q2 Q4 and Q6. The three-legged bridge is designed to carry current from phases P, Q, and R of the alternating current grid. Two MOSFETs with antiparallel make up each leg of the bridge and are driven by corresponding pulses. Each leg (P, Q, R) of the full-bridge circuit is connected to one of three MOSFETs through antiparallel and that are connected in series with the inductor. Three symmetric reference waves with a phase difference of 120 degrees are initially generated within the control module of the intended ANFIS-GA controller H6 fed to inverter to generate adequate driving pulses for the MOSFETs of the full-bridge circuit. The BLDC motor reference signal is compared to zero to produce driving pulses. The driving pulses for the three-phase bridge switches are generated by turning each leg of

the entire bridge ON while the associated reference signal is greater than or equal to the width of the trapezoidal pulse to attain desired output.

4. Result and discussion

ANFIS-GA control methodology is implemented in MATLAB/Simulink to control BLDC drive as shown in Figure 6. At the initial stage of simulation, we generate PWM signal which is suitable for BLDC control. As a result, motor speed is regulated, and controller is wired to receive the hall signal which can detect its rising and falling point position of the BLDC's rotor. The controller uses the rotor rising and falling point position of the hall signals as inputs to perform a combinational logic calculation that generates the rotor speed. Hall sensor is used for combining the balanced Hall signals with an efficient ANFIS-GA controller to enhance PWM signal according to the BLDC drive. In order to regulate the motor speed, the speed controller still determines by the duty ratio of the efficient PWM signal.

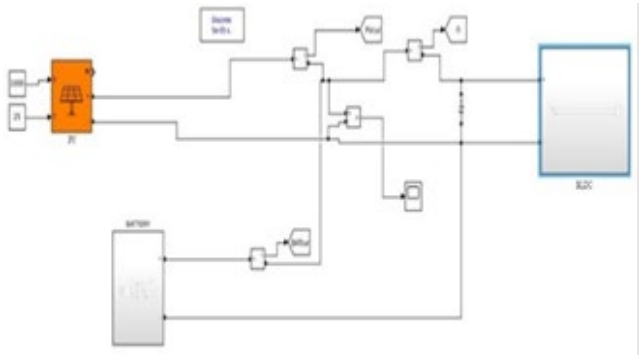

Figure 6. MATLAB simulation for hybrid input source fed BLDC motor

During secondary stage of simulation, ANFIS-GA torque controller is then used to generate objective based PWM signals based on the initial PWM signal and the balanced Hall signals. A logical circuit of the microcontroller is used to implement the logical signal to the H6 inverter as illustrated in Figure 7. Whereas only the lower bridge switches are affected by the PWM delay while operating in high bridge switching PWM mode operation.

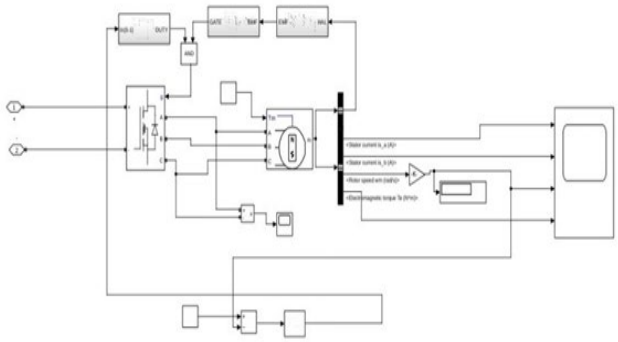

Figure 7. MATLAB simulation of sub-system for hybrid input source fed inverter to drive BLDC motor

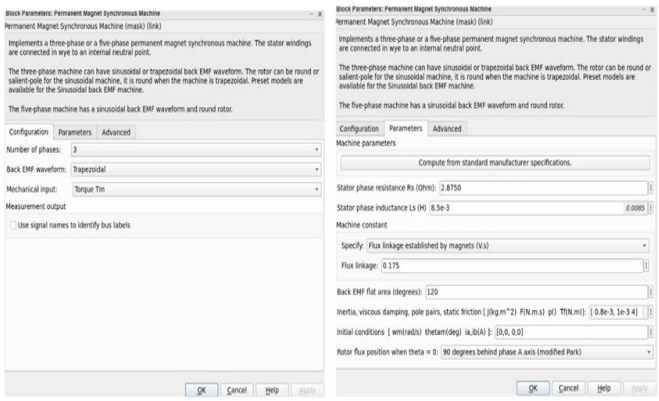

Figure 8. MATLAB simulation for BLDC motor parameters

As a result, the BLDC motor's speed range and efficiency are improved with the provided parameters as shown in Figure 8. After consisting comparative speed (RPM) and settling time analysis, it was determined that all three algorithms, GA (Genetic Algorithm), ABC (Artificial Bee Colony), and GSO (glowworm swarm optimization), would be compared on the factor of run time. The comprehensive results of the GA, ABC and GSO algorithms are displayed in Figure 9, and which illustrated the maximum run duration achieved before settling down to the nominal speed. The graphical comparison result demonstrates that the GA performs better than the other two methods algorithm. It is obvious that the GA works better. The GA also proves to be superior in terms of speed, which means that the GA can be utilized as a dominant for ANFIS to solve variety of optimization problems. Hence, we conclude that to attain significant and most optimal solution in a predetermined amount of time, given that GA requires less time than ABC and GSO to generate an optimal or near-optimal solution. Similarly, stator current also considered after the above analysis. ABC and GSO algorithms attained their peak current usage before dropping down to their regular rates. The GA visually outperforms the other two algorithms, explaining its selection. Despite its speed

advantage, the GA can also be utilized to invalidate BLDC stator wining heat problems during the long run and improve efficiency.

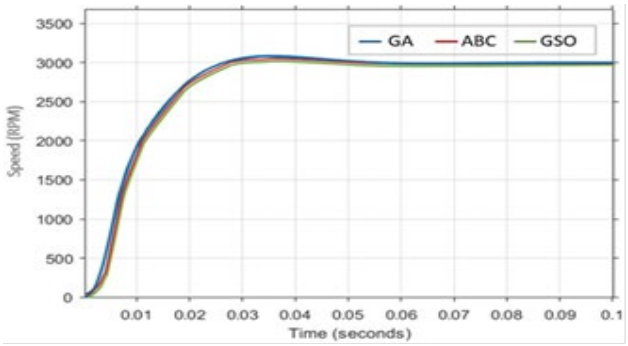

Figure 9. Comparison of GA, ABC, GSO

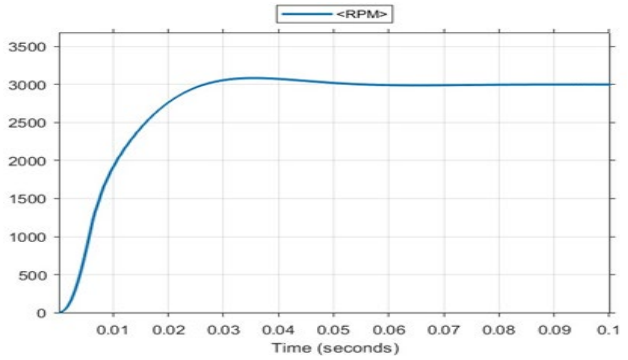

Figure 10. MATLAB simulation outcome for BLDC motor

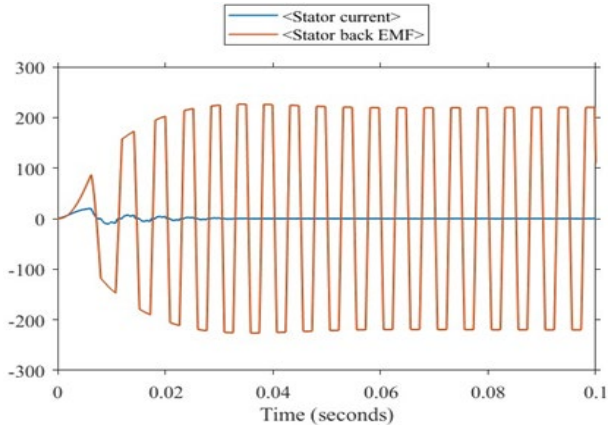

Figure 11. Simulated output of stator current and stator back EMF

As proven in Figure 10 & Figure 11, provided a seamless transition at rated 3000 RPM speed, the duty ratio of MOSFET switch is modified to maintain a constant dc-link voltage. Using a hardware model, the hybrid input source fed H6 inverter is design for controlling BLDC motor drive was verified. From Figure 12, it is clearly stated the hybrid input source fed to inverter could be utilized during the transitional phase of low-speed operation of BLDC motor drive. The H6 Inverter has a faster response time than other converters utilized in such schemes.

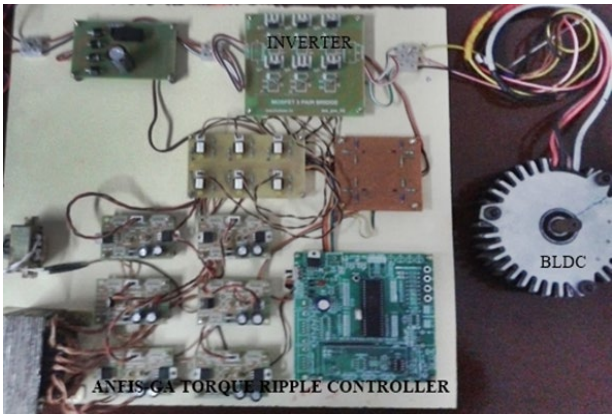

Figure 12. Hardware for inverter fed BLDC motor drive

The hardware results for the BLDC motor at rated voltage 500W and rated speed of 3000RPM. Hall sensors are used for measuring voltage and current, and hall sensors with feedback connections inside the motor's stator are used to calculate speed. The ANFIS-GA controller board algorithm is programmed, and torque of the load is modulated using hall sensor at load side system. For the identical operating conditions, the BLDC motor's phase current, torque, and speed responses are carried out. The results show that the trapezoidal waveform is very ideal, and that the torque ripple is minimized across the 3000RPM speed range.

5. Conclusion

The proposed circuit methodology is experimented to significantly enhance the BLDC motor control drive's performance. According to the findings, the proposed implemented of a GA trained ANFIS system strategy is both effective and reliable. The suggested torque controller circuit offers several benefits over the previously investigated methodology for eliminating torque ripple. 1) The drive can operate the BLDC motor at its rated conditions with a lower hybrid input supply voltage. 2) The torque controller drive system is efficient and generate efficient PWM signal to the H6 Voltage Source Inverter. When the rated voltage of the motor is greater than the hybrid PV-Battery supply voltage, the proposed inverter methodology will benefit the drive system. The proposed circuit methodology is shown to greatly enhance the BLDC drive's performance and stability. For BLDC drives using ANFIS-GA controller, research suggests a torque ripple compensation. The effectiveness of the torque ripple compensation has been demonstrated both in simulation and in practice. The proposed ANFIS-GA torque controller drive reduces torque ripple and BLDC motor attains its efficient rated

speed around 3000RPM as shown in the experimental discussion.

References

[1] Geetha A, Subramani C. A. Comprehensive review on energy management strategies of hybrid energy storage system for electric vehicles. Int. J. Energy Res. 2017; 41(13):1817-1834.

[2] Aloo LA, Kihato PK, Kamau SI, Orenge RS. Interleaved boost converter voltage regulation using hybrid ANFIS-PID controller for off-grid microgrid. BEEI. 2023; 12(4):2005-2016.

[3] Khan H, Khatoon S, Gaur P, Khan SA. Speed control comparison of wheeled mobile robot by ANFIS, Fuzzy and PID controllers. Int. J. Inf. Technol. 2022; 14(4):1893-1899.

[4] Prajapati A, Tiwari P. Design and Simulation of ANFIS based Brushless DC Motor Control. Samriddhi - j. phys. sci. eng. technol. 2021; 13(02):70-76.

[5] Anbazhagan G, Jayakumar S, Muthusamy S, Sundararajan SCM, Panchal H, Sadasivuni KK. An effective energy management strategy in hybrid electric vehicles using Taguchi based approach for improved performance. Energy Sources A: Recovery Util. Environ. Eff. 2022; 44(2):3418-3435.

[6] Iqubal M, Stonier AA, Vanaja DS, Peter G. Design of a modular converter in hybrid EV charging station with efficient energy management system. Electr. Eng. 2023; 1(3):1-20.

[7] Abdelfattah H, Mosaad MI, Ibrahim NF. Adaptive neuro fuzzy technique for speed control of six-step brushless DC motor. Indones. J. Electr. Eng. Inform. 2021; 9(2): 302-312.

[8] Subramani S, Vijayarangan KK, Chenniappan M. Improved African Buffalo Optimization-Based Takagi–Sugeno–Kang Fuzzy PI Controller for Speed Control in BLDC Motor. Electr. Power Compon. Syst. 2023; 1(2): 1-15.

[9] Gharajeh MS, Jond HB. An intelligent approach for autonomous mobile robot's path planning based on adaptive neuro-fuzzy inference system. Ain Shams Eng. J. 2022; 13(1):101-491.

[10] Dasari M, Reddy AS, Kumar MV. A comparative analysis of converters performance using various control techniques to minimize the torque ripple in BLDC drive system. SUSCOM. 2022; 33(1):100-648.

[11] Jegajothi B, Geethamahalakshmi G, Raja A, Mahendran N. An efficient metaheuristic optimization based fuzzy controller for brushless DC drives lifetime expansion. Mater. Today: Proc. 2022; 56(5):3343-3348.

[12] Okoji AI, Anozie AN, Omoleye JA. Evaluating the thermodynamic efficiency of the cement grate clinker cooler process using artificial neural networks and ANFIS. Ain Shams Eng. J. 2022; 13(5):101-704.

[13] Gayatri Sarman KVSH, Madhu T, Mallikharjuna Prasad A. Fault diagnosis of BLDC drive using advanced adaptive network-based fuzzy inference system. Soft Comput. 2021; 25(20):12759-12774.

[14] Bharanigha V, Shuaib YM. Minimization of torque ripples with optimized controller based four quadrant operation & control of BLDC motor. Adv. Eng. Softw. 2022; 172(1):103-192.

[15] Kannan R, Sundharajan V. A novel MPPT controller based PEMFC system for electric vehicle applications with interleaved SEPIC converter. Int. J. Hydrog. Energy. 2023; 48(38):14391-14405.